Journal of the American College of Cardiology
© 2008 by the American College of Cardiology Foundation
Published by Elsevier Inc.

Vol. 52, No. 10, 2008
ISSN 0735-1097/08/$34.00
doi:10.1016/j.jacc.2008.05.038

Electroanatomic Characterization of Post-Infarct Scars

Comparison With 3-Dimensional Myocardial Scar Reconstruction Based on Magnetic Resonance Imaging

Andrei Codreanu, MD,*§ Freddy Odille, MS,§ Etienne Aliot, MD,* Pierre-Yves Marie, MD, PHD,†‖ Isabelle Magnin-Poull, MD,* Marius Andronache, MD,* Damien Mandry, MD,‡ Wassila Djaballah, MD,†§ Denis Régent, MD,‡§ Jacques Felblinger, PHD,§ Christian de Chillou, MD, PHD*§

Nancy, France

Objectives This study was designed to compare electroanatomic mapping (EAM) and magnetic resonance imaging (MRI) with delayed contrast enhancement (DCE) data for delineation of post-infarct scars.

Background Electroanatomic substrate mapping is an important step in the post-infarct ventricular tachycardia (VT) ablation strategy, but this technique has not yet been compared with a gold-standard noninvasive tool informing on the topography and transmural extent of myocardial scars in humans.

Methods Ten patients (9 men, age 71 ± 10 years) admitted for post-infarct VT ablation underwent both a left ventricle DCE MRI and a sinus-rhythm 3-dimensional (3D) (CARTO) EAM (Biosense Webster, Johnson & Johnson, Diamond Bar, California). A 3D color-coded MRI-reconstructed left ventricular endocardial shell was generated to display scar data (intramural location and transmural extent). A matching process allocated any CARTO point to its corresponding position on the MRI map. Electrogram (EGM) characteristics were then evaluated in relation to scar data.

Results A spiky EGM morphology, a reduced unipolar or bipolar EGM voltage amplitude (<6.52 and <1.54 mV, respectively), as well as a longer bipolar EGM duration (>56 ms) independently correlated with the presence of scar whatever its intramural position. Endocardial scars had a larger degree of signal reduction than intramural or epicardial scars. None of the parameters was correlated with transmural scar depth. A clear mismatch in infarct surface between CARTO and MRI maps was observed in one-third of infarct zones.

Conclusions Sinus-rhythm EAM helps identify the limits of post-infarct scars. However, the accuracy of EAM for precise scar delineation is limited. This limit might be circumvented using anatomical information provided by 3D MRI data. (J Am Coll Cardiol 2008;52:839–42) © 2008 by the American College of Cardiology Foundation

Substrate mapping is recognized as an important step in the post-infarct ventricular tachycardia (VT) ablation strategy (1). Electroanatomic mapping (EAM) helps to delineate post-infarct scars, but this technique has not yet been compared with a noninvasive gold-standard tool, such as magnetic resonance imaging (MRI) with delayed contrast enhancement (DCE), informing on the topography and transmural extent of myocardial scars in humans (2). The aim of this study was to obtain 3-dimensional (3D) MRI reconstructions of the left ventricle (LV) showing the location and transmural extent of the infarction and to compare these data with 3D electroanatomic sinus-rhythm LV maps in patients undergoing a post-infarct VT ablation procedure.

Methods

Patients. Ten consecutive patients (9 men, age 71 ± 10 years) with a history of remote (14 ± 9 years) myocardial infarction, referred for catheter ablation of sustained monomorphic VT, underwent cardiac MRI study before the ablation procedure. The study was performed after informed consent and according to institutional guidelines on ethics and methodology of clinical investigation.

MRI acquisition and analysis. Electrocardiogram (ECG)-triggered MRI sequences were recorded on a 1.5-T system (Signa Excite, GE, Waukesha, Wisconsin). The DCE images were acquired after intravenous injection

From the Departments of *Cardiology, †Nuclear Medicine, and ‡Radiology and §IADI INSERM ERI 13, University Hospital Nancy, Nancy, France; and the ‖UHP-INSERM 684, Medicine School, Nancy, France.

Manuscript received December 18, 2007; revised manuscript received April 22, 2008, accepted May 20, 2008.

JACC Vol. 52, No. 10, 2008
September 2, 2008:839–42

Abbreviations and Acronyms

DCE = delayed contrast enhancement
EAM = electroanatomic mapping
ECG = electrocardiogram
EGM = electrogram
LV = left ventricle
MRI = magnetic resonance imaging
ROC = receiver-operator curve
3D = 3-dimensional
VT = ventricular tachycardia

of 0.1 mmol/kg body weight gadolinium-diethylenetriamine penta-acetic acid (Magnevist, Schering AG, Berlin, Germany) using a short-axis multislice 3D segmented inversion-recovery gradient-echo pulse sequence with effective slice thickness ≤5 mm. A 3D ventricular reconstruction was obtained offline using a homemade application in the MATLAB environment (Mathworks, Natick, Massachusetts). Left ventricular endocardial/epicardial and scar contours were manually defined on contiguous short-axis slices using computer-assisted calipers (Fig. 1). Orthogonal long-axis views were used to cross-check for scar location and extent. Atrioventricular annuli and the aortic root were the anatomical landmarks. Analysis was performed automatically according to a radial segmentation map consisting of a 32-radii grid perpendicular to the LV long axis and centered on it. On the basis of manually outlined contours, the location and transmural extent of the scar were calculated along each radius. A 3D endocardial shell reconstruction of the LV was then generated and color-coded to provide information as to infarct location and depth as follows: epicardial scars in blue; intramural scars in dark green; endocardial to transmural scars from yellow to orange, then red; and healthy myocardium in pale green.

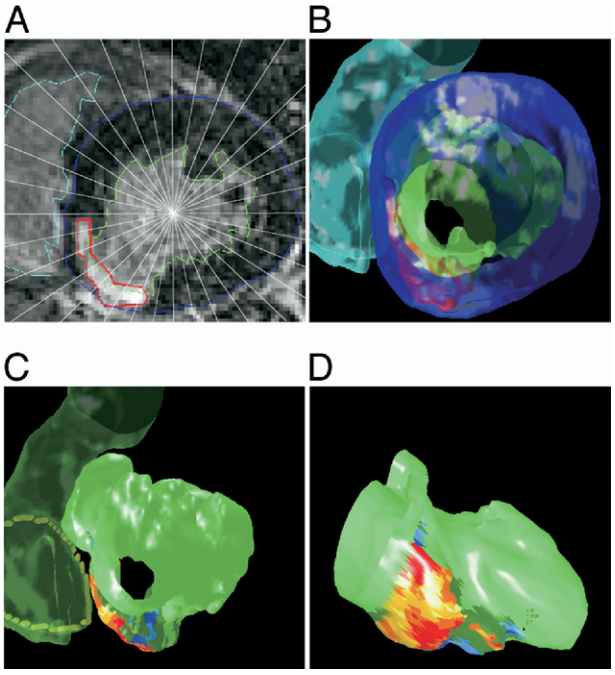

Figure 1 **Three-Dimensional LV Reconstruction Based on MRI Data**

(A) Short-axis view centered on the left ventricle (LV) with the 32 radial sectors grid and the manually drawn contours of the LV endocardium **(green)**, LV epicardium **(dark blue)**, and LV scar **(red)**. **(B)** Endocardial and epicardial LV volumes and scar volume are automatically reconstructed using an isosurface algorithm. **(C and D)** Resulting color-coded three-dimensional map (**C**, left anterior oblique view; **D**, right anterior oblique view) of the LV endocardial surface: **pale green** represents healthy tissue whereas **other colors** indicate myocardial infarction with various intramural involvements. MRI = magnetic resonance imaging.

3D EAM. Using a previously described technique (3), all patients underwent LV 3D mapping using the CARTO system (Biosense Webster, Johnson & Johnson, Diamond Bar, California). Briefly, the LV was plotted during sinus rhythm by dragging a 3.5 mm irrigated-tip 7-F mapping/ablation catheter (NAVI-STAR, Cordis-Webster, Johnson & Johnson, Baldwin Park, California) over the endocardium, with more points acquired in infarct areas. The left atrioventricular junction was carefully mapped to delineate the mitral annulus. Filter bandpass settings were 1 to 240 Hz and 30 to 400 Hz for unipolar and bipolar electrograms (EGMs), respectively.

Data collected for each LV sinus rhythm EGM were: 1) unipolar voltage amplitude; 2) bipolar voltage amplitude; 3) bipolar voltage duration (time from first to the last sharp component of the EGM, measured at a time scale of 200 mm/s); 4) spiky bipolar EGM (presence of more than 4 sharp spikes within an EGM, with baseline crossing between them); 5) fractionated bipolar EGM (amplitude <0.5 mV, duration >133 ms, and/or amplitude/duration ratio <0.005); and 6) double-potentials bipolar EGM (2 distinct potentials ≥50 ms aside, with a return to baseline between them).

Comparison between CARTO maps and MRI data. Using anatomical landmarks (mitral annulus plane, LV apex, and aortic root), an offline matching process was performed between the MRI and the CARTO maps, allowing each CARTO map point to be allocated in a corresponding MRI slice (in the LV short-axis view) and finally a radial sector. The characteristics of any EGM could thus be evaluated in relation to the presence of scar, to intramural location, and to transmural scar extent on its ascribed MRI zone.

Given the absence of consensus on bipolar voltage criteria for post-infarct substrate mapping (4,5), CARTO voltage maps obtained using different bipolar EGM voltage cutoff values (<0.5, <1.5, and <2.0 mV) were compared with the corresponding infarct surface automatically measured on the MRI-reconstructed map.

Statistical analysis. Results are expressed as mean ± SD, unless otherwise specified. To account for the correlation between EGM characteristics and MRI scar, multivariate logistic regression and chi-square tests were performed (SAS/STAT, version 8.2, SAS Institute, Inc., Cary, North Carolina). Comparison between scar areas on MRI maps and low-voltage areas in CARTO used distribution free statistical tests: 2-tailed Mann-Whitney *U* tests and chi-square or Fisher exact tests when appropriate. A p value <0.05 was considered statistically significant.

Results

The DCE MRI identified 4 LV anterior scars and 8 LV inferior scars in the 10 patients. Sub-endocardial to transmural scars predominated (80 ± 6% of the total infarct surface projected onto the endocardium). Usually located at the infarct border, intramural and epicardial scars were present in all patients (14 ± 4% and 6 ± 5% of total infarct surface, respectively).

Endocardial scar depth was 34 ± 7% of the wall thickness, with 80 ± 8% of scars involving <3/4 of wall thickness.

Of the 1,045 CARTO map points (85 to 190 per patient), 561 were ascribed in a MRI area with endocardial scar, 27 in a zone with intramural or epicardial scar, and 457 points in noninfarcted myocardium.

All morphologically abnormal EGM parameters were significantly ($p < 0.0001$) more prevalent in scars compared with healthy areas: spiky EGM (78.6% vs. 18.6%), fractionated EGM (43.2% vs. 6.8%), and double-potentials EGM (11.2% vs. 3.5%). Significantly ($p < 0.001$) lower bipolar (0.97 ± 1.09 mV vs. 3.20 ± 2.61 mV) and unipolar (4.80 ± 2.38 mV vs. 10.29 ± 5.09 mV) EGM voltages, as well as longer EGM durations (81.57 ± 37.94 ms vs. 42.60 ± 21.75 ms), were also found in scars versus healthy areas. Using receiver-operator curve (ROC) area measurements, threshold values best predicting the presence of scar were as follows: 6.52 mV for unipolar EGM voltage (ROC area: 0.87), 1.54 mV for bipolar EGM voltage (ROC area: 0.85), and 56 ms for bipolar EGM duration (ROC area: 0.83). Multivariate stepwise logistic regression found 4 parameters independently correlated with the presence of scar: a spiky EGM morphology, a reduced unipolar or bipolar EGM voltage, and a longer bipolar EGM duration. The statistical model including all 4 parameters resulted in a 0.9 ROC area. No correlation was found between any EGM parameter and transmural scar extent.

Bipolar EGM amplitude was the only parameter showing a significant ($p < 0.007$) difference between endocardial and intramural/epicardial scars (0.94 ± 1.07 mV vs. 1.52 ± 1.41 mV).

The MRI-reconstructed infarct surfaces best correlated to CARTO infarct areas defined by a <1.5 mV bipolar cutoff value ($r^2 = 0.82$, $p < 0.0001$) compared with <0.5 ($r^2 = 0.57$, $p = 0.043$) and <2 mV ($r^2 = 0.67$, $p = 0.0012$) limits. When using the 1.5 mV cutoff, a mismatch >20% in infarct surface measurement was observed in 4 of 12 scar areas (33%), with the presence of scar zones not confirmed on MRI views in 3 cases and underestimation of the infarct surface in the fourth. Among the different EGM parameters, a <6.5 mV unipolar voltage best correlated ($r^2 = 0.86$, $p < 0.0001$) with the presence of scar on MRI.

Because precise scar border delineation may be clinically relevant for VT ablation purposes, scar morphology on the color-coded MRI map was compared with the corresponding infarct area on the CARTO 1.5 mV bipolar voltage map. Controlled identical anatomical

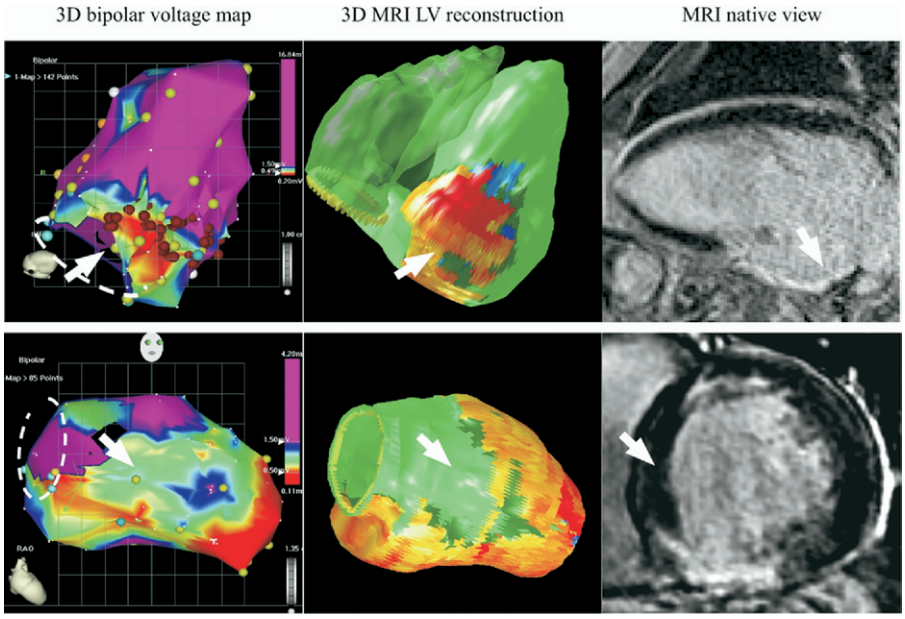

Figure 2 **Mismatch in Scar Delineation Between CARTO Bipolar Maps and MRI Shells**

(Left) CARTO bipolar maps; **(middle)** MRI shells; **(right)** native MRI images. The **top row** shows underestimated inferior wall scar on the CARTO map. The **bottom row** shows LV septal scar on the CARTO map not confirmed by MRI. On **each panel,** the **arrows** show the mismatch zone. The **dotted lines** represent the mitral annulus plane. 3D = 3-dimensional; other abbreviations as in Figure 1.

projections of the 2 3D reconstructions were used. A clear mismatch was found in 4 of 12 (33%) infarct areas (Fig. 2), with presence of 3 scar areas not confirmed on the MRI views (basal LV septum 2 cases, inferior-basal 1 case), whereas in 1 case, the CARTO map underestimated the infarct surface (inferior-basal) compared with MRI reconstruction.

Discussion

Sinus-rhythm EAM was found to identify infarct areas in animal models (4,5). In human studies (1,6,7), however, high-density EAM scar definition using multiple EGM parameters has never been matched against a gold-standard technique based on tissue characterization. This comparison was first evaluated in the present study, which confirmed that bipolar EGM characteristics can reliably differentiate scar from healthy tissue.

Additionally, our data suggest that a combination of these parameters would further increase infarct area definition. However, parameters such as EGM duration or the presence of spiky potentials can hardly be automatically measured online, which precludes their use in clinical practice so far.

Our data show that bipolar voltage analysis, in opposition to unipolar analysis, could help identify scar areas with intramural/epicardial location. Compared with unipolar recording, bipolar recording more accurately reflects local changes in electrical activity and is less influenced by far-field electrical activity (8), possibly explaining its ability to provide information about intramural scar location. Our study also found that EGM characteristics were unable to predict transmural scar depth, and contradictory data exist in articles on this subject (7,9). The inability of EGM to predict transmural scar depth suggests the potential utility of complementary MRI anatomical information in scar definition.

Most importantly, this study first shows that 3D EAM, compared with DCE MRI, provides only a rough delineation of infarct areas. Mismatch typically occurred in regions (basal LV septum and posterior wall) where achievement of catheter stability and a good wall contact are technically challenging via the trans-aortic approach. As a consequence, lower density of recorded points and/or acquisition of erroneous EGM signals would result in a wrong definition of scar contours.

Conclusions

Our study confirms that sinus-rhythm EAM helps to identify the limits of post-infarct scar. A precise scar description cannot, however, be guaranteed by electroanatomic data. Anatomical information provided by 3D MRI data may be of interest to improve scar definition. Whether this would be clinically relevant needs further evaluation.

Reprint requests and correspondence: Dr. Christian de Chillou, Département de Cardiologie - CHU de Nancy, 54511 Vandoeuvre les Nancy Cedex, France. E-mail: c.dechillou@chu-nancy.fr.

REFERENCES

1. Marchlinski FE, Callans DJ, Gottlieb CD, Zado E. Linear ablation lesions for control of unmappable ventricular tachycardia in patients with ischemic and nonischemic cardiomyopathy. Circulation 2000;101:1288–96.
2. Wu E, Judd RM, Vargas JD, Klocke FJ, Bonow RO, Kim RJ. Visualisation of presence, location, and transmural extent of healed Q-wave and non-Q-wave myocardial infarction. Lancet 2001;357:21–8.
3. de Chillou C, Lacroix D, Klug D, et al. Isthmus characteristics of reentrant ventricular tachycardia after myocardial infarction. Circulation 2002;105:726–31.
4. Callans JD, Ren J-F, Michele J, Marchlinski F, Dillon S. Electroanatomic left ventricular mapping in the porcine model of healed anterior myocardial infarction. Correlation with intracardiac echocardiography and pathological analysis. Circulation 1999;100:1744–50.
5. Wrobleski D, Houghtaling C, Josephson ME, Ruskin J, Reddy V. Use of electrogram characteristics during sinus rhythm to delineate the endocardial scar in a porcine model of healed myocardial infarction. J Cardiovasc Electrophysiol 2003;14:524–9.
6. Reddy VY, Neuzil P, Taborski M, Ruskin JN. Short-term results of substrate-mapping and radiofrequency ablation of ischemic ventricular tachycardia using a saline-irrigated catheter. J Am Coll Cardiol 2003;41:2228–36.
7. Perin EC, Silva GV, Sarmento-Leite R, et al. Assessing myocardial viability and infarct transmurality with left ventricular electromechanical mapping in patients with stable coronary artery disease: validation by delayed-enhancement magnetic resonance imaging. Circulation 2002;106:957–61.
8. Wit AL, Janse MJ. Extracellular electrograms and mode of recording: unipolar, bipolar and composite electrograms. In: The Ventricular Arrhythmias of Ischemia and Infarction: Electrophysiological Mechanisms. Mount Kisco, NY: Futura Publishing Company, 1993:225–31.
9. Wolf T, Gepstein L, Dror U, et al. Detailed endocardial mapping accurately predicts the transmural extent of myocardial infarction. J Am Coll Cardiol 2001;37:1590–17.

Key Words: myocardial infarction ■ ventricular tachycardia ■ magnetic resonance imaging ■ electrophysiology ■ catheter ablation.